RESEARCH REPORT VTT-R-00901-22

TUTTE Project Final Report

Authors: Manu Huttunen
Timo Karlsson
Jennifer Carreiro Spencer
Raul Prieto

Confidentiality: VTT Public

Version: 02.11.2022

beyond the obvious

Report's title	
Final Report	
Customer, contact person, address Business Finland, Joint Action (Co-Innovation)	**Order reference** N.A.
Project name Tuulivoiman tuotanto ja tehokkuus	**Project number/Short name** 126473 / TUTTE
Author(s) Manu Huttunen, Timo Karlsson, Jennifer Carreiro Spencer, Raul Prieto	**Pages** 25/
Keywords Wind Energy, Wind Inflow, Wake Effects, Atmospheric Stability, Efficiency, Icing, Modelling	**Report identification code** VTT-R-00901-22

Summary

In the public research part of the TUTTE joint action, atmospheric conditions were measured by field campaigns carried out in an onshore and in an offshore wind farm located in Finland. Lidar measurements of wind flow, measurements of ambient temperature and pressure at hub height and ground level, and wind turbine SCADA data were analysed. Wind speed, wind shear and turbulence intensity along with seasonal variability of the wind at these two sites was investigated. Atmospheric stability was estimated by three different metrics. Diurnal and seasonal variability of potential temperature difference, which is included in two of the metrics, was explored. Wind farm wake effects and production losses due to wakes, topography and icing were analysed, and the influence of atmospheric stability on wind farm efficiency was examined. The offshore wind farm was modelled by open-source tools developed by The National Renewable Energy Laboratory (NREL) and the model was validated against wind farm SCADA data. VTT's research team collaborated with Stanford University and NREL.

Confidentiality	VTT Public

Espoo 4.11.2022

Written by	Reviewed by
Manu Huttunen, Senior Scientist	Raul Prieto, Team Leader

VTT's contact address
P.O. Box 1000, FI-02044 VTT, Finland

Distribution (customer and VTT)

To be published at VTT Research Information Portal.

Approval

VTT TECHNICAL RESEARCH CENTRE OF FINLAND LTD

Date:	04.11.2022
Signature:	DocuSigned by: Raul Prieto FA1A895B52D447F...
Name:	Raul Prieto
Title:	Research Team Leader

Preface

Co-innovation project Tuulivoiman tuotanto ja tehokkuus (TUTTE) funded by Business Finland was conducted between 3.8.2020 and 2.11.2022. The goal of the joint action TUTTE was to produce new knowledge on factors contributing to and limiting the energy production of wind farms in Finnish climate. The focus was on seasonal and diurnal effects on wind flow, wind farm efficiency, wakes and contribution of surrounding terrain to wind farm efficiency. Measurements relating to icing conditions were collected.

To achieve these goals, the joint action was implemented in close collaboration with Finnish companies, and wind farm owners and operators. To enable the research projects of the joint action partners, two field measurement campaigns were executed. These campaigns were conducted in operating wind farms, one at an offshore location and another one onshore. Research data was also generated by means of simulations. International collaboration partners were Stanford University in California and The National Renewable Energy Laboratory in Colorado.

The project steering group included Allwinds Ab and EPV Tuulivoima Oy, their support in data collection is greatly appreciated. Other steering group companies were Flexens Oy, Numerola Oy (merged to AFRY Finland Oy during the project) and Wicetec Oy.

Espoo 02.11.2022

Authors

Contents

Preface 3
1. Introduction 5
2. Generation of data 5
   2.1 Båtskär, Allwinds 5
   2.2 Santavuori, EPV 6
   2.3 Wind farm modelling 7
   2.4 Summary of the data 7
3. Methods 9
   3.1 Atmospheric conditions and wind farm efficiency 9
   3.2 Wake effects 9
   3.3 Icing 10
   3.4 Wind farm modelling 12
4. Results 14
   4.1 Atmospheric conditions and wind farm efficiency 14
   4.2 Wake losses 14
   4.3 Icing at Santavuori wind farm 16
      4.3.1 Production loss due to icing 16
      4.3.2 Icing conditions 17
   4.4 Modelling Båtskär wind farm 20
5. Business case analysis 22
   5.1 Analysing wake losses 22
   5.2 Increasing efficiency of wind energy 22
   5.3 Spinning-off TwinThrive 22
6. IEA collaboration 23
7. Conclusions 23
References 24

1. Introduction

With the current energy crisis in Europe and the increasing demand for renewable energy to combat global warming, the role of wind energy in the energy mix and the production efficiency of wind power is ever more important. Distinguished scientists and industry members in the field of wind energy highlight as one of three grand challenges of the field the improved understanding of the physics of atmospheric flow in the critical zone of wind power plant operation [1]. They see the characterization of lower atmosphere where wind turbines operate is essential for both designing turbines of the future and for dynamic control of the machines.

Influence of atmospheric stability on the wind flow downstream of an operational wind turbine, i.e. the wake, has attracted more and more attention in the research community. It has been found that wind speed, wind shear, wind veer, turbulence and thermal stratification of the region of atmospheric boundary layer where the turbines operate in influence the wake behaviour [2]–[11] not forgetting the surrounding terrain [12], [13].

In this project, the wind flow observed by field measurement campaigns carried out in an onshore and in an offshore wind farm located in Finland is characterized. Lidar measurements of wind flow, measurements of ambient temperature and pressure at hub height and ground level, and wind turbine SCADA data is analysed. Wind speed, wind shear and turbulence intensity along with seasonal variability of the wind at these two sites is investigated. Atmospheric stability is estimated by three different metrics. Diurnal and seasonal variability of potential temperature difference, which is included in two of the metrics, is explored. Wind farm wake effects and production losses due to wakes, topography and icing are analysed, and the influence of atmospheric stability on wind farm efficiency is examined. The Båskär wind farm is modelled by open-source tools developed by The National Renewable Energy Laboratory (NREL) and the model is validated against wind farm SCADA data.

Overall information of data generated in this project is given in Section 2. Information describing the methods utilized in this work is laid out in Section 3. Research results are summarised in Section 4. Overview of business case analysis is given in Section 5 and of IEA collaboration in Section 6. Finally, conclusions about project results are presented in Section 7.

2. Generation of data

Wind flow was observed by two field measurement campaigns carried out in Allwinds' Båtskär wind farm in Åland and EPV's wind farm located in Santavuori, Finland. More detailed wind farm descriptions and instrumentation listings are published in a scientific article by the Authors in collaboration with Stanford University [14].

2.1 Båtskär, Allwinds

The Båtskär wind farm in Lemland, Åland comprises of six Enercon E70 2.3MW wind turbines based on small islets 16 km south of Mariehamn. Figure 1 illustrates the location of the wind farm and turbine layout.

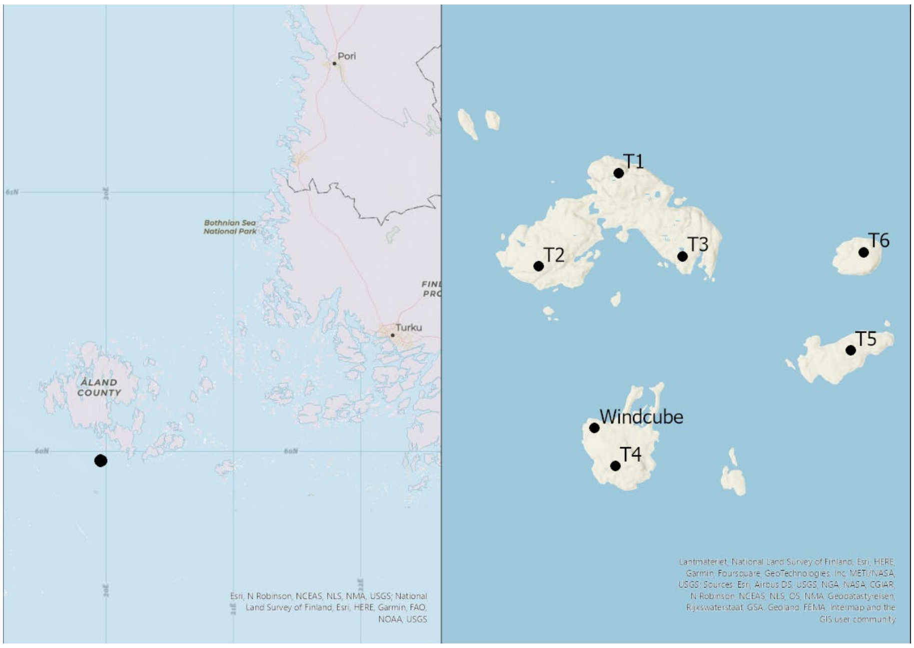

Figure 1. Båtskär wind farm location and turbine layout.

The Båtskär wind farm has a rated capacity of 14 MW. The hub height of the six 2.3 MW wind turbines is 68 meters and the rotor diameter is 70 meters. Turbines #1 and #2 are instrumented with the sensing equipment described in the instrumentation summary. SCADA data is collected from all turbines.

Maximum elevation on the islets from the average sea level is 10 meters. All turbines lie within 558 meters radius. Distances between closest neighbouring turbines range from 314 to 689 meters i.e., from 4.5D and 9.8D.

A summary of the measurement instruments installed which relate to inflow characterisation directly or via estimation is presented in

Table 1.

Table 1. Summary of measurements relevant to inflow at Båtskär wind farm.

Location	Measurement instrumentation	Notes
Turbine 1	Nacelle-mounted forward-facing LIDAR Ambient air measurement Turbine electric generator signals Blade bending strain measurements	 Voltages and currents Edgewise and flapwise
Turbine 2	Nacelle-mounted forward-facing LIDAR Nacelle-mounted backward-facing LIDAR Turbine electric generator signals Blade bending strain measurements	 Voltages and currents Edgewise and flapwise
Lilla Båtskär	Windcube vertical profiling LIDAR	

2.2 Santavuori, EPV

Santavuori wind farm is located eight kilometres south from the city centre of Ilmajoki, Finland comprises of 17 Vestas 3.3 MW wind turbines. Figure 2 depicts the location of the wind farm and layout of turbines.

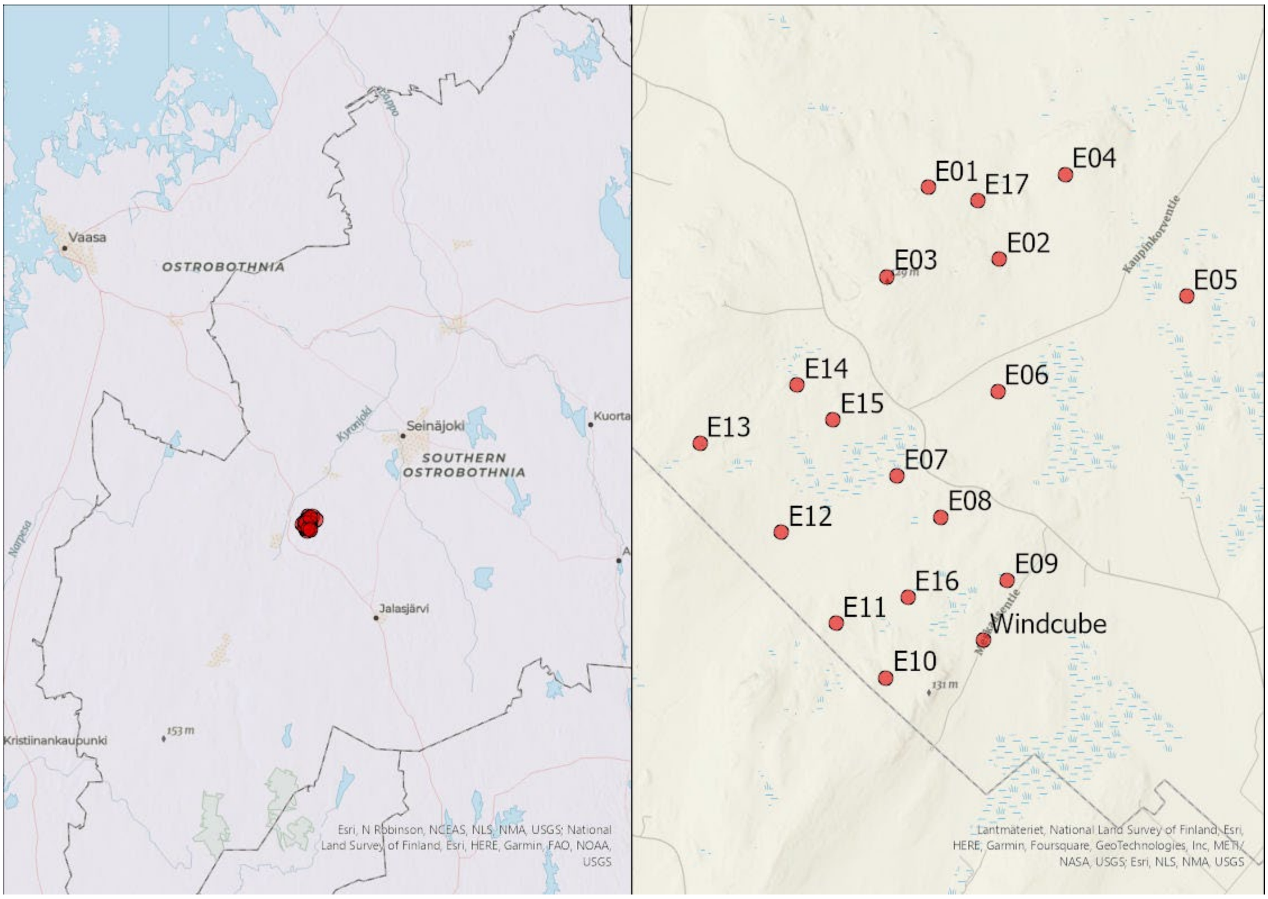

Figure 2. Santavuori wind farm location and turbine layout.

Hub height is 137 meters and rotor diameter 126 meters. Turbine E12 is instrumented with nacelle mounted lidars. The following figure illustrates the layout of the Santavuori wind farm, along with the corresponding identification for each turbine. Table 2 list measurement devices used at this site.

Table 2. Summary of measurements relevant to inflow at Santavuori wind farm.

Location	Measurement instrumentation	Notes
Turbine E12	Nacelle-mounted forward-facing LIDAR Nacelle-mounted backward-facing LIDAR	
Near E9 & E16	Windcube vertical profiling LIDAR	
Near E9 & E16	Ceilometer	

2.3 Wind farm modelling

Simulation codes and tools developed by NREL were used to model Båtskär wind farm. The Enercon E70 wind turbine was modelled with OpenFAST simulation software. Individual turbine models were compiled in wind farm setting using FAST.Farm code. Wind flow fields were generated with TurbSim.

2.4 Summary of the data

Devices used in field measurement campaigns and recorded signals with their sampling rates are summarised in Table 3 and Table 4 for Båtskär and Santavuori wind farms respectively.

Table 3. Summary of field measurement devices and signals at Båskär wind farm and their sampling rates.

Data source	Length	Sampling rate	Contents	Notes
Båtskär SCADA	2019-2022	10 min	SCADA data for 6 turbines	
Windcube	Dec. 2020-Dec. 2021	1 min	Wind at 10 heights	
Lidar 1	Dec. 2020-Dec. 2021	1 Hz / 10 min	Wind in front of rotor	Turbine 1 facing forward
Lidar 2	Dec. 2020-Dec. 2021	1 Hz / 10 min	Wind in front of rotor	Turbine 2 facing forward
Lidar 3	Dec. 2020-Dec. 2021	1 Hz / 10 min	Wind turbine wake	Turbine 2
Blade loads	Dec. 2020-Dec. 2021	200 Hz	Flapwise and edgewise strain	All blades, turbine 1 and 2
Blade root temperature	Dec. 2020-Dec. 2021	1 Hz	Temperature at the location of the strain gauges	Only one blade
Blade A pitch angle	Dec. 2020-Dec. 2021	10 Hz	Encoder installed at root of blade A to measure pitch angle	
Tower loads	Sep. 2021-Dec. 2021	10 Hz	North-south and east-west strain	
Vibrations	Dec. 2020-Dec. 2021	10 Hz	Nacelle vibrations in two dimensions	Two turbines
Current and voltage	Dec. 2020-Dec. 2021	500 Hz	Generator current and voltage	Turbines 1 and 2
Rotor position	Dec. 2020-Dec. 2021	500 Hz	Two different types of encoders installed in the nacelle to measure rotor rotation Pulse per rotation & pulse per mechanical lock slot in the rotor	Actual position / azimuth angle needs to be separately calculated.
Weather	Dec. 2020-Dec. 2021	1 Hz	Temperature, relative humidity, temperature	Nacelle top of turbine 1

Table 4. Summary of field measurement devices at Santavuori wind farm and their sampling rates.

Data source	Length	Sampling rate	Contents	Notes
SCADA	Jan 2019 - Mar 2022	10 min	SCADA data from 17 turbines	
Lidar 1	Dec 2020 – Nov 2021	1 Hz / 10min	Wind in front of rotor	Installed on turbine 12
Lidar 2	Dec 2020 – Nov 2021	1 Hz / 10min	Turbine wake	Installed on turbine 12
Vertical lidar	Dec 2020 – Nov 2021	1 minute	Wind at 10 levels	
Ceilometer	Jan 2021 – Apr 2022	1 minute	Cloud base height	

3. Methods

Overview of methods used in the research is presented below. More detailed description of methods mentioned in Section 3.1 is presented in [14] and for Section 3.2 in [15].

3.1 Atmospheric conditions and wind farm efficiency

Analysis of inflow wind and atmospheric stability was carried out using lidar measurements. Characteristics such as rotor equivalent wind speed, wind shear, turbulence intensity for wind, and environmental lapse rate (ELR), Brunt-Väisälä frequency and Bulk Richardson number for stability estimation were computed. Influence of atmospheric stability on production efficiency of Santavuori wind farm was examined by comparing daytime and night-time efficiencies.

3.2 Wake effects

The quantification of wind farm wake losses is challenging because of the many factors affecting the data collected in wind farm SCADA. Operational factors include curtailments, wind turbine warnings and pauses in operation. Atmospheric factors include performance degradation due to icing, as well as gradual effect of blade erosion. All these factors result in wind turbines operating in abnormal conditions.

Finally, the orography of the site produces a non-homogeneous flow field which generates a distortion of the air velocity as a function of wind direction.

It was formulated as a research question that the effect of orography in overall wind farm efficiency can be comparable to the effect of wakes, and therefore an estimation of wake losses using SCADA would require a process to estimate the wind farm efficiency by separating the effect of the orography from the effect of the wakes.

To address this research question, a method has been developed to identify the separate the contributions to wind farm efficiency produced by the site orography and the interaction of wind turbine wakes. The dataset compiled from Santavuori wind farm has been used to produce this method, which is described in detail in [15].

The following steps have been used to produce the analysis:

1) Merging of wind farm SCADA data with Vertical wind profiling LIDAR data (Windcube), which was available for the period 2020-12-01 through 2021-11-04.

2) Filtering of dataset to discard abnormal operating conditions for all the wind turbines. This is done by comparing the average SCADA blade pitch against the expected blade pitch corresponding to the nacelle wind conditions. Further, potential icing events which could distort wake loss estimate are removed by discarding low temperatures.

3) Identification of upstream wind turbines not affected by wakes, based on Windcube wind direction.

4) Identification of wake impingement events and turbine efficiency using the Jensen model.

5) Estimation of individual wind turbine efficiency for each downstream wind turbine (i.e. ratio of power between the downstream turbine and the consensus upstream turbines).

6) Averaging of wind turbine efficiencies to obtain the overall wind farm efficiency for each time step.

7) Averaging of wind farm efficiencies across all time steps.

During step 5, a correction of the individual wind turbine efficiency may be applied, based on the relations among the upstream turbines and the downstream turbine. The formulation of the correction and its effect on the estimated efficiency is presented in [15].

The datasets obtained are described below in Section 4 *Results*.

3.3 Icing

When air temperature drops below zero degrees centigrade, cloud droplets can still remain in liquid form. When these supercooled droplets collide with a wind turbine blade, ice can form on the turbine blade. Icing on the blade can increase the aerodynamic drag of the blade and decrease the lift generated by the blade leading to production losses. This process is known as in-cloud icing.

When assessing icing conditions, it is important to make a difference between meteorological icing, weather conditions when ice can form, and rotor icing, the actual period when ice is present on the surface of the blade (see Figure 3). These are linked, but they are not the same.

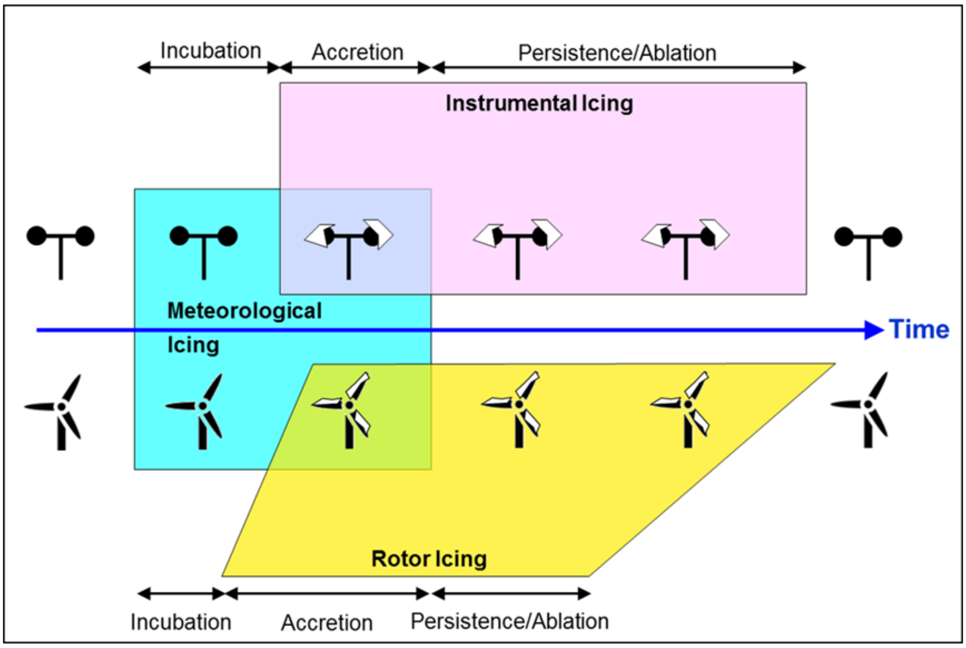

Figure 3. The different stages of an icing event [16].

Santavuori site is at a location that does suffer from blade icing to a degree. The severity of this icing impact can be estimated from weather models or weather observations. Specific icing atlases also exist for Finland that can be used to get an idea of the icing conditions at the site.

VTT world icing atlas (WIceAtlas) is one example. WIceAtlas is based on cloud base height measurements over a long period of time and can be used to assess the frequency of in-cloud icing at site. [17]

WIceAtlas gives an estimate of 2.9% of icing annually. IEA wind Task 19 has published a site icing classification that can be used as a reference when assessing icing conditions at a site (Table 5) [18]. The 2.9 % meteorological icing given by the VTT WIceAtlas would put this site in ice class 2. Based on this, the expected production losses due to icing would be below 5 % of annual energy production.

Table 5. IEA ice classification.

IEA Ice Class	Duration of Meteorological Icing [% of Year]	Duration of Instrumental Icing [% of Year]	Production Loss [% of AEP]
5	>10	>20	>20
4	5-10	10-30	10-25
3	3-5	6-15	3-12
2	0.5-3	1-9	0.5-5
1	0-0.5	<1.5	0-0.5

Impact of blade icing can be calculated from SCADA data based on production loss as compared to wind speeds in comparable conditions at warmer temperatures.Using the Task 19 icelossmethod published by IEA wind Task 19 in 2017, the relative losses can be estimated for all turbines separately [19]. The solution here relies on a "clean, warm weather" reference that is calculated directly from the data. Then the full dataset is compared to this reference and potential icing cases are marked.

The clean reference is made by taking the fraction of the data, where the ambient temperature at the nacelle level is above 3 °C. This dataset is binned based on wind speed and direction, then for each bin a P10 value (10th percentile) is calculated. The threshold for icing is that if the output power is below this limit continuously for an hour and temperature is below 1 °C, the reason for the drop in power is assumed to be icing.

In comparison to this power curve-based method, there was also a ceilometer at the site. Using the ceilometer information of cloud base height and the nacelle level temperature information, it is possible to calculate the number of hours a rotor is inside a cloud, or a blade passes through a cloud. These can be evidence of in-cloud icing happening.

3.4 Wind farm modelling

Båtskär was chosen as the wind farm site in which to perform a validation by using simulations, specifically with FAST.Farm. These simulations were conducted within a multi-tool framework developed by NREL (National Renewable Energy Laboratories). The main tools used for the simulations include BModes, TurbSim, OpenFAST and FAST.Farm. FAST.Farm is a mid-fidelity tool for modelling the effects of turbine wakes across a wind farm. [20] Each turbine model in FAST.Farm is developed in OpenFAST, which accurately models the turbine aerodynamic, structural and control / electrical dynamics in a coupled process. [21] BModes is another in the toolset developed by NREL, which looks at the modal shapes and frequencies of turbine blades and tower. [22] Lastly, FAST.Farm allows coupling with a precursor simulation designed to generate inflow data. Some of these include SOWFA, which is a high-fidelity boundary layer solver and TurbSim, a synthetic turbulence generator. [23], [24]

The first step was to create an accurate model of the turbine, in this case the Enercon E70, in the OpenFAST environment. Due to not having knowledge of every turbine parameter, these needed to be deduced for the model. Firstly, this involved extracting the blade geometry from images taken of the turbine. Subsequently, the blade and tower stiffness values were examined from the strain gauges installed on both the tower and blades. From the strain gauges, installed at 90-degree intervals around the cross sections, the edgewise and flapwise natural frequencies were found. An approximation of these natural frequencies was achieved iteratively by using the BModes tool. By gradually adjusting the stiffness parameters for the blades and tower, the output modal shapes and frequencies were approximated to the experimental data obtained from the strain gauges. As the last step, the controller for the wind turbine model was implemented using NREL's Reference OpenSource Controller (ROSCO) toolset. With the finished model of the Enercon E70 turbine, a series of simulations were run with OpenFAST to generate an output of the power curve. This could then be compared to the reference data sheet values as well as the data obtained from the measurement campaign at Båtskär.

With a completed turbine model, some initial tests were performed with FAST.Farm without using a precursor inflow generator. In this case, FAST.Farm applies a simple uniform flow without the need for additional simulations. FAST.Farm combines various modules created by NREL to derive the power performance and structural loads of turbines situated in a wind farm.

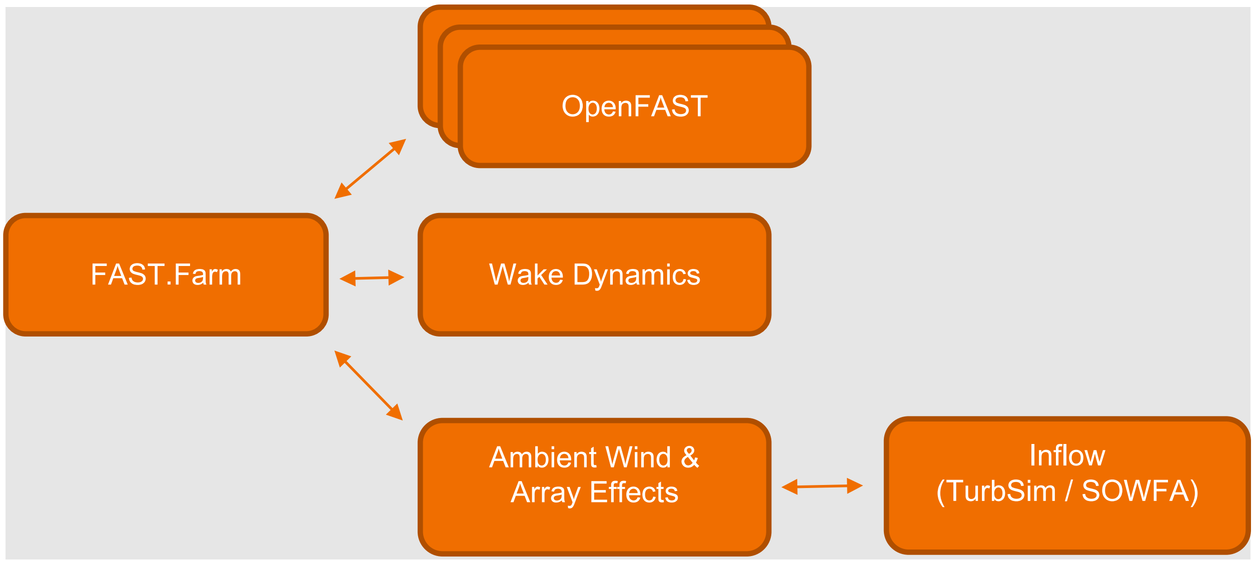

Figure 4. Basic schematic of FAST.Farm environment. [20]

Initially, the inflow was generated by using SOWFA, a high-fidelity solver for the atmospheric boundary layer. After preliminary testing with this tool, it was deemed too computationally expensive to achieve a validation across a wide range of atmospheric conditions. Additionally, it is highly complex which increases the difficulty to understand and utilise this tool. A different inflow solver (AMRWind) is being developed and in the future will be coupled for use with FAST.Farm.

A second and faster option for generating the FAST.Farm ambient wind precursor is TurbSim. This does not fully resolve the atmospheric boundary layer, but instead is a turbulence simulator which generates inflows with relevant fluid dynamics to evaluate turbine response. [23]

The experimental data collected during the Båtskär campaign was then filtered to provide a set of conditions to be used as inputs for TurbSim. These were points where quasi-steady wind conditions were present in a full-impingement scenario where Turbine 1 is affected by the wake of Turbine 2, or vice versa. Filters are also applied to limit the wind speed, turbulence and shear range. Given the specifications of the wind farm and inflow conditions, a TurbSim simulation low-resolution domain is created which encompasses the entire set of turbines. After this, the timeseries of this simulation is extracted before feeding this as an input for a high-resolution simulation around each turbine. Combining the outputs from both these low and high-resolution TurbSim precursor simulations provides the inflows for the FAST.Farm simulations. [20]

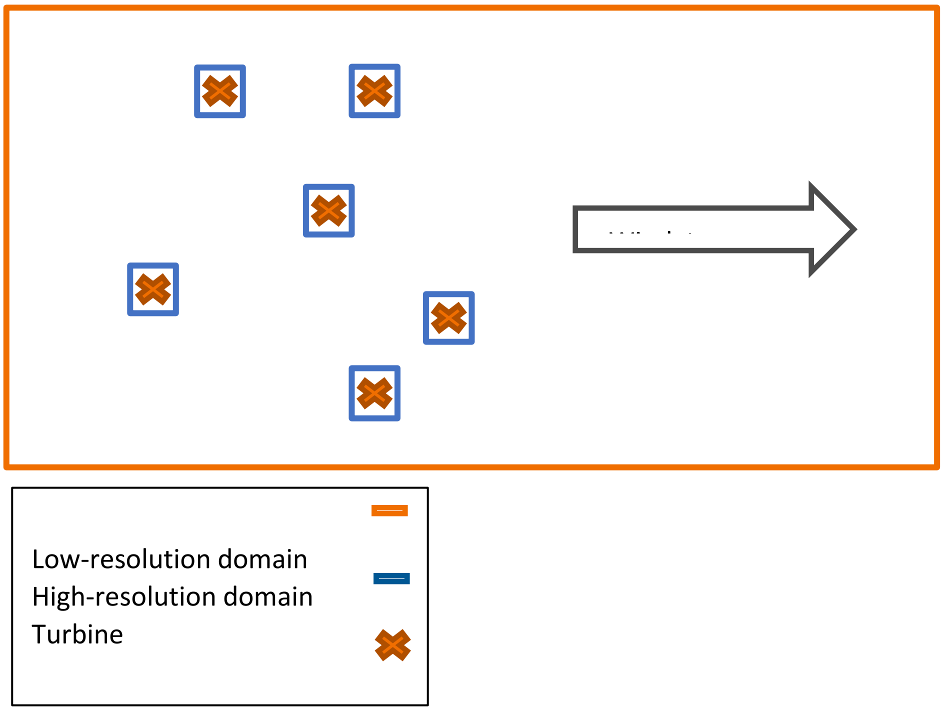

Figure 5. FAST.Farm and TurbSim domains with turbine locations. [20]

Alongside the generated low and high-resolutions inflows, parameters are taken from the TurbSim simulations which then are used to produce the main FAST.Farm input files. From the results of FAST.Farm, the operational performance of the turbines under the varied inflow conditions can be analysed and compared to the reference data.

4. Results

4.1 Atmospheric conditions and wind farm efficiency

During the field measurement campaigns, average monthly wind speeds vary between 6.0 and 11 m/s for Båtskär and from 5.5 to 8.2 m/s for Santavuori, summer months of June and July recording the lowest averages. Wind shear and turbulence intensities are higher for Santavuori most likely due to the influence of the forestry terrain and hills surrounding this site. Overall, similar seasonal and diurnal trends for potential temperature difference between the hub height and ground level were observed for both wind farm locations, but at Båskär this difference showed more variation during two winter months. Again overall, comparison of the stability metrics computed for the two wind farm locations suggest on average more stable stratification for Santavuori. Average wind farm production losses are greater for Santavuori wind farm because of denser layout of the wind farm. Comparing wind farm efficiency of Santavuori between daytime and night-time during summer, reveals a noticeable effect of stability on wind farm losses. For a more elaborated account on the results the reader is directed to [14].

4.2 Wake losses

Two datasets were generated by combining SCADA, Lidar and the Jensen wake model. They are referred as “Level 1” (L1):

The *Level 1 (L1) - Wake interaction dataset* : Contains for every 10-minute time step the following data:

1) Upstream wind speed, direction and electric power from consensus upstream turbines,
2) contemporaneous Windcube speed and direction,
3) number of wakes impinging the incumbent wind turbine according to Jensen wake model, and designation of offending turbines,
4) experimental efficiency of the incumbent wind turbine, and
5) efficiency predicted with Jensen wake model using different wake decay coefficients.

The *Level 1 (L1) – Wind power plant dataset*: Contains for every 10-minute time step the following data:

1) Wind farm power and wind farm reference upstream power,
2) efficiency once removed the effect of orography,
3) sum of all offending turbines using the Jensen wake model, and

also items 1) and 2) from the wake interaction dataset.

1	datetime	waked Turbine	w_ref [m/s]	winddir_ref [deg]	TI_ref [-]	dens-ref [kg/m3]	ws_wc [m/s]	wd_wc [deg]	TI_wc [-]	T_air_wc [degC]	pair [mbar]	shearexp_wc [-]	Pasquill
2	08/12/2020 09:50	1	7.25	140.721	0.09655	1.2877	7.1705	140.721	0.12854	-1.8	1011.53	0.47643	6
3	08/12/2020 09:50	2	7.25	140.721	0.09655	1.2877	7.1705	140.721	0.12854	-1.8	1011.53	0.47643	6
4	08/12/2020 09:50	3	7.25	140.721	0.09655	1.2877	7.1705	140.721	0.12854	-1.8	1011.53	0.47643	6
5	08/12/2020 09:50	4	7.25	140.721	0.09655	1.2877	7.1705	140.721	0.12854	-1.8	1011.53	0.47643	6
6	08/12/2020 09:50	5	7.25	140.721	0.09655	1.2877	7.1705	140.721	0.12854	-1.8	1011.53	0.47643	6
7	08/12/2020 09:50	6	7.25	140.721	0.09655	1.2877	7.1705	140.721	0.12854	-1.8	1011.53	0.47643	6
8	08/12/2020 09:50	7	7.25	140.721	0.09655	1.2877	7.1705	140.721	0.12854	-1.8	1011.53	0.47643	6
9	08/12/2020 09:50	8	7.25	140.721	0.09655	1.2877	7.1705	140.721	0.12854	-1.8	1011.53	0.47643	6
10	08/12/2020 09:50	9	7.25	140.721	0.09655	1.2877	7.1705	140.721	0.12854	-1.8	1011.53	0.47643	6
11	08/12/2020 09:50	10	7.25	140.721	0.09655	1.2877	7.1705	140.721	0.12854	-1.8	1011.53	0.47643	6
12	08/12/2020 09:50	11	7.25	140.721	0.09655	1.2877	7.1705	140.721	0.12854	-1.8	1011.53	0.47643	6
13	08/12/2020 09:50	13	7.25	140.721	0.09655	1.2877	7.1705	140.721	0.12854	-1.8	1011.53	0.47643	6
14	08/12/2020 09:50	14	7.25	140.721	0.09655	1.2877	7.1705	140.721	0.12854	-1.8	1011.53	0.47643	6
15	08/12/2020 09:50	15	7.25	140.721	0.09655	1.2877	7.1705	140.721	0.12854	-1.8	1011.53	0.47643	6
16	08/12/2020 09:50	16	7.25	140.721	0.09655	1.2877	7.1705	140.721	0.12854	-1.8	1011.53	0.47643	6
17	08/12/2020 09:50	17	7.25	140.721	0.09655	1.2877	7.1705	140.721	0.12854	-1.8	1011.53	0.47643	6
18	08/12/2020 10:00	1	7.16	139.764	0.10056	1.2883	6.758	139.764	0.12331	-1.8	1011.6	0.44113	6
19	08/12/2020 10:00	2	7.16	139.764	0.10056	1.2883	6.758	139.764	0.12331	-1.8	1011.6	0.44113	6
20	08/12/2020 10:00	3	7.16	139.764	0.10056	1.2883	6.758	139.764	0.12331	-1.8	1011.6	0.44113	6
21	08/12/2020 10:00	4	7.16	139.764	0.10056	1.2883	6.758	139.764	0.12331	-1.8	1011.6	0.44113	6
22	08/12/2020 10:00	5	7.16	139.764	0.10056	1.2883	6.758	139.764	0.12331	-1.8	1011.6	0.44113	6
23	08/12/2020 10:00	6	7.16	139.764	0.10056	1.2883	6.758	139.764	0.12331	-1.8	1011.6	0.44113	6
24	08/12/2020 10:00	7	7.16	139.764	0.10056	1.2883	6.758	139.764	0.12331	-1.8	1011.6	0.44113	6
25	08/12/2020 10:00	8	7.16	139.764	0.10056	1.2883	6.758	139.764	0.12331	-1.8	1011.6	0.44113	6
26	08/12/2020 10:00	9	7.16	139.764	0.10056	1.2883	6.758	139.764	0.12331	-1.8	1011.6	0.44113	6
27	08/12/2020 10:00	10	7.16	139.764	0.10056	1.2883	6.758	139.764	0.12331	-1.8	1011.6	0.44113	6
28	08/12/2020 10:00	11	7.16	139.764	0.10056	1.2883	6.758	139.764	0.12331	-1.8	1011.6	0.44113	6
29	08/12/2020 10:00	13	7.16	139.764	0.10056	1.2883	6.758	139.764	0.12331	-1.8	1011.6	0.44113	6
30	08/12/2020 10:00	14	7.16	139.764	0.10056	1.2883	6.758	139.764	0.12331	-1.8	1011.6	0.44113	6
31	08/12/2020 10:00	15	7.16	139.764	0.10056	1.2883	6.758	139.764	0.12331	-1.8	1011.6	0.44113	6
32	08/12/2020 10:00	16	7.16	139.764	0.10056	1.2883	6.758	139.764	0.12331	-1.8	1011.6	0.44113	6
33	08/12/2020 10:00	17	7.16	139.764	0.10056	1.2883	6.758	139.764	0.12331	-1.8	1011.6	0.44113	6
34	08/12/2020 10:10	1	7.32	139.378	0.10656	1.2883	7.2625	139.378	0.12553	-1.76	1011.6	0.38076	6
35	08/12/2020 10:10	2	7.32	139.378	0.10656	1.2883	7.2625	139.378	0.12553	-1.76	1011.6	0.38076	6

1	power_ref [kW]	power_waked [kw]	power_ratio [-]	power_ratio_JK [-]	cp	ct	ct_ideal	n_offending	n_offending_JK	list_of_offending_WECs	list_of_offending_WECs_JK
2	1261.32	1465.8	1.1621	0.4621	0.47912	0.7604	0.58197	2	1	2,6	2
3	1261.32	1257.8	0.99721	1	0.41113	0.76786	0.47722	0	0	0	0
4	1261.32	1471.8	1.1669	0.54316	0.48108	0.76019	0.58526	3	1	6,8,9	6
5	1261.32	1418	1.1242	1	0.4635	0.76211	0.55641	1	0	5	0
6	1261.32	1199.4	0.95091	1	0.39204	0.76995	0.45025	0	0	0	0
7	1261.32	1371.8	1.0876	1	0.4484	0.76377	0.53266	0	0	0	0
8	1261.32	1373	1.0885	0.43783	0.44879	0.76373	0.53326	2	1	8,9	8
9	1261.32	1523.8	1.2081	0.4171	0.49808	0.75836	0.61461	1	1	9	9
10	1261.32	1281.5	1.016	1	0.41888	0.76701	0.48842	0	0	0	0
11	1261.32	1533.2	1.2156	1	0.50115	0.75803	0.6201	0	0	0	0
12	1261.32	1418	1.1242	0.43947	0.4635	0.76211	0.55641	1	1	10	10
13	1261.32	2329	1.8465	-9999	0.76127	0.73361	1.0221-0.	5	3	9,10,11,1	10,11,12
14	1261.32	974.8	0.77284	0.60241	0.31863	0.77817	0.3532	6	1	7,8,9,10,1	15
15	1261.32	1068.8	0.84737	0.61171	0.34936	0.77473	0.39269	4	1	7,8,9,16	7
16	1261.32	1039.4	0.82406	1	0.33975	0.7758	0.38018	0	0	0	0
17	1261.32	270.7	0.21462	1	0.08848	0.8192	0.09058	2	0	2,5	0
18	1212.04	1382	1.1402	0.47728	0.46878	0.76341	0.56493	3	1	2,5,6	2
19	1212.04	1564.7	1.291	1	0.53075	0.75693	0.67673	0	0	0	0
20	1212.04	1526.7	1.2596	0.48991	0.51786	0.75826	0.65113	2	1	6,9	6
21	1212.04	1519	1.2533	0.51066	0.51525	0.75853	0.64613	1	1	5	5
22	1212.04	1396.3	1.152	1	0.47363	0.76289	0.57286	0	0	0	0
23	1212.04	1170.8	0.96597	1	0.39714	0.771	0.45736	0	0	0	0
24	1212.04	1165.4	0.96152	0.51444	0.39531	0.77119	0.4548	2	1	8,9	8
25	1212.04	1161.1	0.95797	0.56454	0.39385	0.77135	0.45276	1	1	9	9
26	1212.04	1196	0.98677	1	0.40568	0.77007	0.46943	0	0	0	0
27	1212.04	1252	1.033	1	0.42468	0.76806	0.49691	0	0	0	0
28	1212.04	1102.2	0.90938	0.5643	0.37387	0.7735	0.42531	1	1	10	10
29	1212.04	2211.8	1.8249	-9999	0.75025	0.73695	1.0138-0.	5	3	9,10,11,1	10,11,12
30	1212.04	793.6	0.65476	0.66739	0.26919	0.78579	0.29241	6	1	7,8,9,10,1	15
31	1212.04	1051.2	0.8673	0.60271	0.35657	0.77537	0.40218	4	1	7,8,9,16	7
32	1212.04	1045.1	0.86227	1	0.3545	0.77559	0.39945	0	0	0	0
33	1212.04	333.6	0.27524	1	0.11316	0.8086	0.11667	2	0	2,5	0
34	1291.24	1634.2	1.2656	0.39916	0.51876	0.75449	0.65287	3	1	2,5,6	2
35	1291.24	1533	1.1872	1	0.48664	0.75804	0.59467	0	0	0	0

1	list_of_nacelle_orientations_in_offending_WECS	list_of_relative_wind_directions_in_offending_WECS	relative_wind_direction_in_offended_WEC[deg]	windspeed_in_offended_WEC[m/s]	reference_pc	p10_limit	power_ratio_ORO_removed[-]	list_distances_to_offending_WECs[Diameters]	list_distances_to_offending_WECs_JK[Diameters]
2	142.020926,140.2	-1.300000,0.5000	0.4	7.5	1398.5	1143.53	1.1434	4.135616e+00,8	4.14E+00
3	-999.9	-999.9	-1.3	7.2	1270.03	1022.95	1.0611	0	4.14E+00
4	140.220926,141.8	0.500000,-1.1000	2.2	7.6	1370.76	1091.45	0.95291	6.510318e+00,1	6.51E+00
5	141.320926	-0.6	-1	7.8	1472.91	1195.42	1.0744	7.01E+00	0
6	-999.9	-999.9	-0.6	7.1	1195.53	976.44	1.0392	0	0
7	-999.9	-999.9	0.5	7.6	1407.61	1169.57	1.1796	0	0
8	141.820926,142.0	-1.100000,-1.3000	-0.1	7.5	1433.55	1163.6	1.1591	2.456119e+00,6	2.46E+00
9	142.020926	-1.3	-1.1	7.8	1535.21	1131.01	1.2014	3.74E+00	3.74E+00
10	-999.9	-999.9	-1.3	7.2	1285.83	1029.97	0.98782	0	3.74E+00
11	-999.9	-999.9	-1.4	8	1585.9	1301.31	1.0948	0	3.74E+00
12	142.120926	-1.4	-1.7	7.6	1474.33	1213.28	1.1267	3.01E+00	3.01E+00
13	142.020926,142.1	-1.300000,-1.4000	0.3	8.7	2186.67	1886.74	1.6621	1.375750e+01,1	1.221554e+01,9.21990
14	140.820926,141.8	-0.100000,-1.1000	-0.3	6.6	947.475	739.285	0.74109	5.510772e+00,7	2.04E+00
15	140.820926,141.8	-0.100000,-1.1000	-1.3	6.7	1053.56	825.072	0.8386	3.474943e+00,5	3.47E+00
16	-999.9	-999.9	0.5	6.6	913.95	-2.78	0.80721	0	3.47E+00
17	142.020926,141.3	-1.300000,-0.6000	0.2	4.3	230.98	120.622	0.22124	2.550586e+00,9	0
18	139.364141,141.1	0.400000,-1.4000	-0.8	7.4	1348.19	1098.63	1.1393	4.135616e+00,1	4.14E+00
19	-999.9	-999.9	0.4	7.7	1537.98	1266.91	1.3959	0	4.14E+00
20	140.364141,141.4	-0.600000,-1.7000	1.2	7.8	1485.68	1188.56	1.0479	6.510318e+00,1	6.51E+00
21	141.164141	-1.4	0	7.9	1528.09	1245.29	1.2141	7.01E+00	7.01E+00
22	-999.9	-999.9	-1.4	7.4	1344.65	1112.61	1.2785	0	7.01E+00
23	-999.9	-999.9	-0.6	7.1	1166.7	949.712	1.0682	0	7.01E+00
24	140.564141,141.4	-0.800000,-1.7000	-0.6	7.2	1284.92	1028.21	1.0376	2.456119e+00,6	2.46E+00
25	141.464141	-1.7	-0.8	7.1	1168.36	575.184	0.96823	3.74E+00	3.74E+00
26	-999.9	-999.9	-1.7	7.1	1235.84	985.556	0.97624	0	3.74E+00
27	-999.9	-999.9	-1.2	7.3	1203.31	946.366	0.93352	0	3.74E+00
28	140.964141	-1.2	-1.8	6.9	1107.14	884.58	0.91213	3.01E+00	3.01E+00
29	141.464141,140.9	-1.700000,-1.2000	-1	8.6	2115.09	1818.25	1.6404	1.375750e+01,1	1.221554e+01,9.21990
30	140.364141,140.5	-0.600000,-0.8000	0.3	6.1	746.38	565.08	0.63128	5.510772e+00,7	2.04E+00
31	140.364141,140.5	-0.600000,-0.8000	-1.8	6.6	1002.78	779.831	0.86529	3.474943e+00,5	3.47E+00
32	-999.9	-999.9	-0.9	6.9	1057.2	-2.72	0.84309	0	3.47E+00
33	139.364141,141.1	0.400000,-1.4000	2	4.6	297.43	174.483	0.28847	2.550586e+00,9	0
34	137.477718,139.7	1.900000,-0.4000	0.6	7.8	1581.74	1312.3	1.2532	4.135616e+00,1	4.14E+00
35	-999.9	-999.9	1.9	7.6	1478.24	1211.69	1.2727	0	4.14E+00

Figure 6. Excerpt from L1 wake interaction dataset, which registers approximately 400k wake interactions among wind turbines.

The wake interaction dataset was filtered to focus on partial production (6-9m/s) and air temperatures above +2C. This subset has approximately 120 000 wake interactions.

A given wind turbine will be operating, with clean inflow between 31%-65% of the time, 20%-26% of the time affected by a single wake, and the rest of the time affected by two or more wakes. The range is due to the criteria defining the wake interaction event, either the Jensen model or geometrical visibility from the downstream turbine looking upwind, using a 55-degree angle.

The presence of a single wake resulted in a drop of efficiency of 3 - 4%; while presence of two wakes increase the drop to 5% - 9%. The average distance between upstream and affected turbines is 8.3 rotor diameters.

Table 6. Time operating in different inflow conditions; and calculated efficiency drop vs. clean inflow. The analysis is limited to partial production 6-9m/s and air temperatures above +2C.

wakes affecting the turbine	fraction of time [%] (Jensen wake criteria, k=0.03)	fraction of time [%] (turbines visible in 55 degree sector ahead)	turbine efficiency drop [%] vs. clean inflow
0 (clean inflow)	65%	31%	-
1	26%	20%	3 - 4%
2	6%	12%	5 - 9%
3	2%	11%	>10%
4 or more	1%	26%	>10%

4.3 Icing at Santavuori wind farm

4.3.1 Production loss due to icing

Based on the power curve using the Task 19 methods it is possible to estimate the production lost due to blade icing. The average for the entire three-year dataset is around 3 % of annual energy production lost due to icing.

This would mean that the site belongs to IEA ice class 2, which given the location makes sense. This does correlate with the estimates that can be had from VTT icing atlas.

Turbine to turbine difference is roughly +- 1 % annually, but year-over-year differences are a lot larger than that. The annual results for each turbine are illustrated in Figure 7.

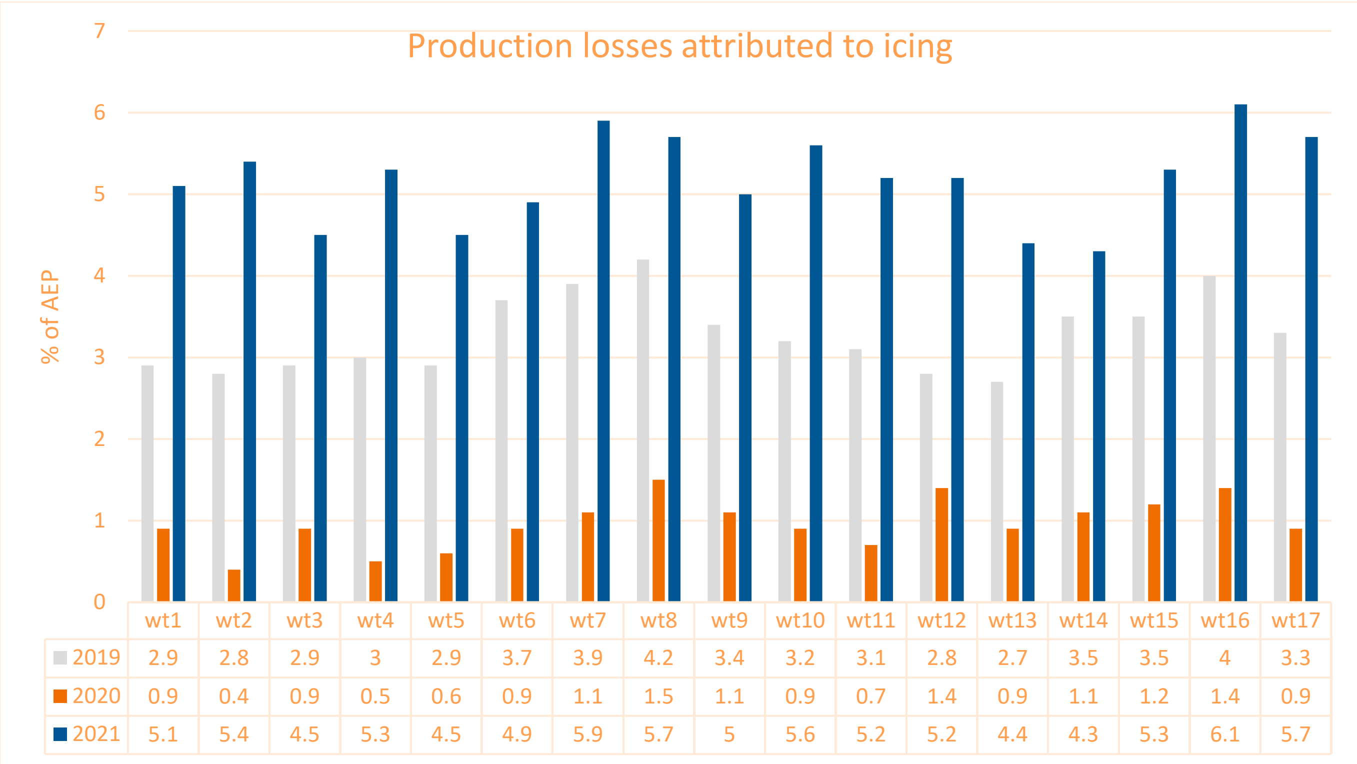

	wt1	wt2	wt3	wt4	wt5	wt6	wt7	wt8	wt9	wt10	wt11	wt12	wt13	wt14	wt15	wt16	wt17
2019	2.9	2.8	2.9	3	2.9	3.7	3.9	4.2	3.4	3.2	3.1	2.8	2.7	3.5	3.5	4	3.3
2020	0.9	0.4	0.9	0.5	0.6	0.9	1.1	1.5	1.1	0.9	0.7	1.4	0.9	1.1	1.2	1.4	0.9
2021	5.1	5.4	4.5	5.3	4.5	4.9	5.9	5.7	5	5.6	5.2	5.2	4.4	4.3	5.3	6.1	5.7

Figure 7. Production losses attributed to icing according to the Task 19 iceloss method. Values are % of AEP.

In this analysis, the year 2020 is a clear outlier, and the icing conditions were significantly less severe in 2020 than during the other two years in the dataset. If icing assessment had been done only based on 2020 data, the conclusions drawn would have been very different from the three-year dataset.

This would suggest that in order to assess icing conditions some kind of long-term assessment would be recommended to catch this variance properly. This can be problematic when doing measurements to assess icing at a site, since the time available for measurement campaigns is limited.

4.3.2 Icing conditions

WiceAtlas also contains information of icing conditions during icing events. These can be compared to similar information extracted from the on-site measurements. Important point here is to note that most of the icing happens at temperatures close to 0 °C and at low wind speeds. (Table 7)

Table 7. Wind speed and temperature during icing conditions in the Wiceatlas database.

	Meteorological icing [% of time]							
winds	**4**	**6**	**8**	**10**	**13**	**16**	**20**	**>20**
temperatures								
-20	0 %	0 %	0 %	0 %				
-15	0 %	0 %	0 %	0 %	0 %			
-10	1 %	2 %	1 %	0 %	0 %	0 %	0 %	0 %
-7	3 %	3 %	2 %	1 %	1 %	0 %	0 %	0 %
-5	2 %	3 %	3 %	1 %	1 %	0 %	0 %	0 %
-3	3 %	5 %	4 %	3 %	1 %	1 %	0 %	0 %
0	10 %	15 %	14 %	8 %	6 %	2 %	1 %	0 %

Similar can be calculated from the turbine results and from the ceilometer measurements. The icing conditions during rotor icing are in Table 8. During rotor icing, if the temperature rises above 0 °C, but the power out continues to be below the P10 level, it is assumed that the icing event continues still, the ice has not been completely removed from the blade. Because of this, a significant subset of the icing events have a temperature above 0 °C.

Table 8. Conditions during rotor icing.

	Rotor icing share					
winds	**4**	**7**	**10**	**13**	**16**	**20**
temperatures						
-15	0.1 %	0.1 %	0.1 %	0.1 %	0.0 %	0.0 %
-10	1.5 %	2.6 %	1.2 %	0.4 %	0.0 %	0.0 %
-7	4.2 %	7.1 %	2.9 %	0.8 %	0.1 %	0.0 %
-5	4.1 %	7.5 %	2.5 %	0.4 %	0.0 %	0.0 %
-3	3.9 %	6.9 %	4.1 %	0.7 %	0.1 %	0.0 %
0	5.4 %	10.5 %	6.8 %	1.3 %	0.4 %	0.2 %
2	4.9 %	11.0 %	6.0 %	1.6 %	0.4 %	0.1 %

Ceilometer was installed on the site next to the vertical wind profiler marked as Windcube in the map in Figure 2. Ceilometer was used as proxy to estimate in-cloud icing by assuming that if cloud base height is below the turbine tip height, there is a risk that the blades can start collecting ice, assuming that the temperature is below 0 °C.

Figure 8 illustrates the estimated meteorological icing time derived from cloud base height measurements and using ambient temperature measured at turbine number 9. (See map in Figure 2).

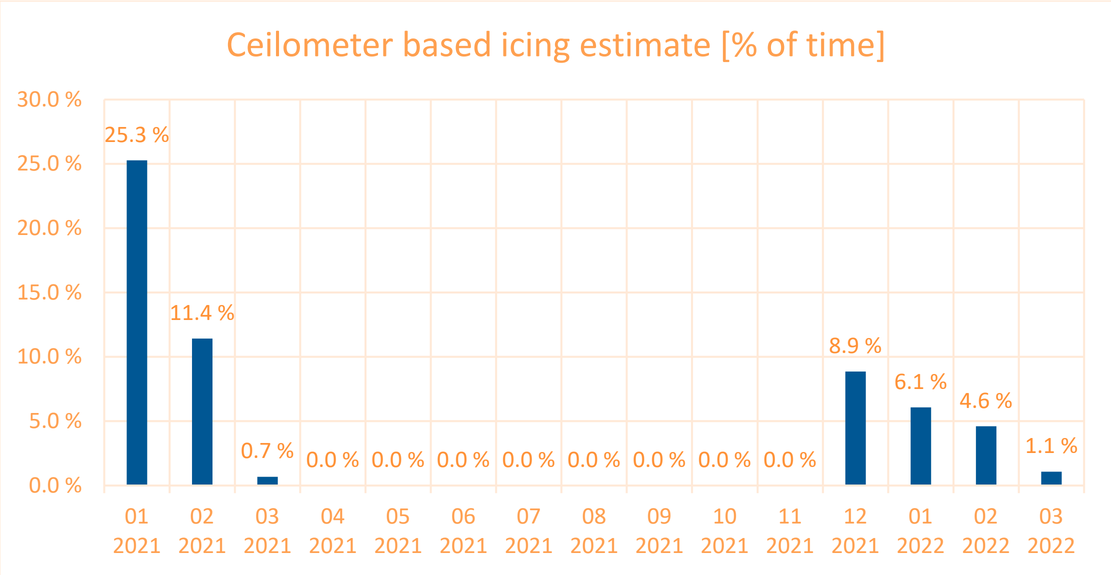

Figure 8. Estimated meteorological icing time (as % of data), estimated from cloud base height measurements.

The annual average for 2021 from this data would be 3.9 % of meteorological icing. This would indicate a slightly higher average icing class than the production losses or the icing atlas. The icing atlas value was 2.9 %. It is possible that the ceilometer data has some amount of false positives due to ice in the clouds. Clouds are not entirely liquid and using the method used here there is no way to tell if the cloud surrounding the rotor is liquid or not. Based on this it can be assumed that at least some of these events did not lead to actual rotor icing.

The conditions during these events are listed in Table 9. There it is visible that the icing events in the ceilometer data happen at a much colder temperature than rotor icing does. This might support the conclusion that there are false positive icing indicators in the ceilometer data.

Table 9. Icing conditions during ceilometer derived icing alerts.

	Icing alarms in ceilometer dataset					
winds	**4**	**7**	**10**	**13**	**16**	**20**
Temperatures						
-15	0.0 %	0.0 %	0.0 %	0.0 %	0.0 %	0.0 %
-10	10.9 %	2.9 %	1.8 %	0.3 %	0.0 %	0.0 %
-7	11.7 %	18.7 %	1.0 %	0.1 %	0.0 %	0.0 %
-5	6.5 %	8.8 %	3.0 %	0.2 %	0.0 %	0.0 %
-3	2.9 %	9.0 %	2.9 %	0.0 %	0.0 %	0.0 %
0	1.8 %	9.5 %	6.8 %	1.0 %	0.0 %	0.0 %
2	0.0 %	0.0 %	0.0 %	0.0 %	0.0 %	0.0 %

There are also some gaps in the ceilometer data. That can affect the average. Fairly significant amount of data is missing in November 2021 and February 2022.

4.4 Modelling Båtskär wind farm

Creating a validated model for the Båtskär wind farm requires a series of sequential steps before achieving a validation on the farm level. This involves first having a validated turbine model for each turbine in the wind farm before beginning with larger-scale multi-turbine simulations.

The first set of results present a validation of the Enercon E70 turbine modelled in OpenFAST. Principally, the power curve is the main indicator in reaching a representative model of the turbine. The figure below shows the comparison between the reference power given in the data sheet and data collected from the Båtskär site in free flow conditions compared to the OpenFAST results for a range of wind velocities. Other parameters to include in the validation include the tip-speed ratio, rotor speed and blade pitch.

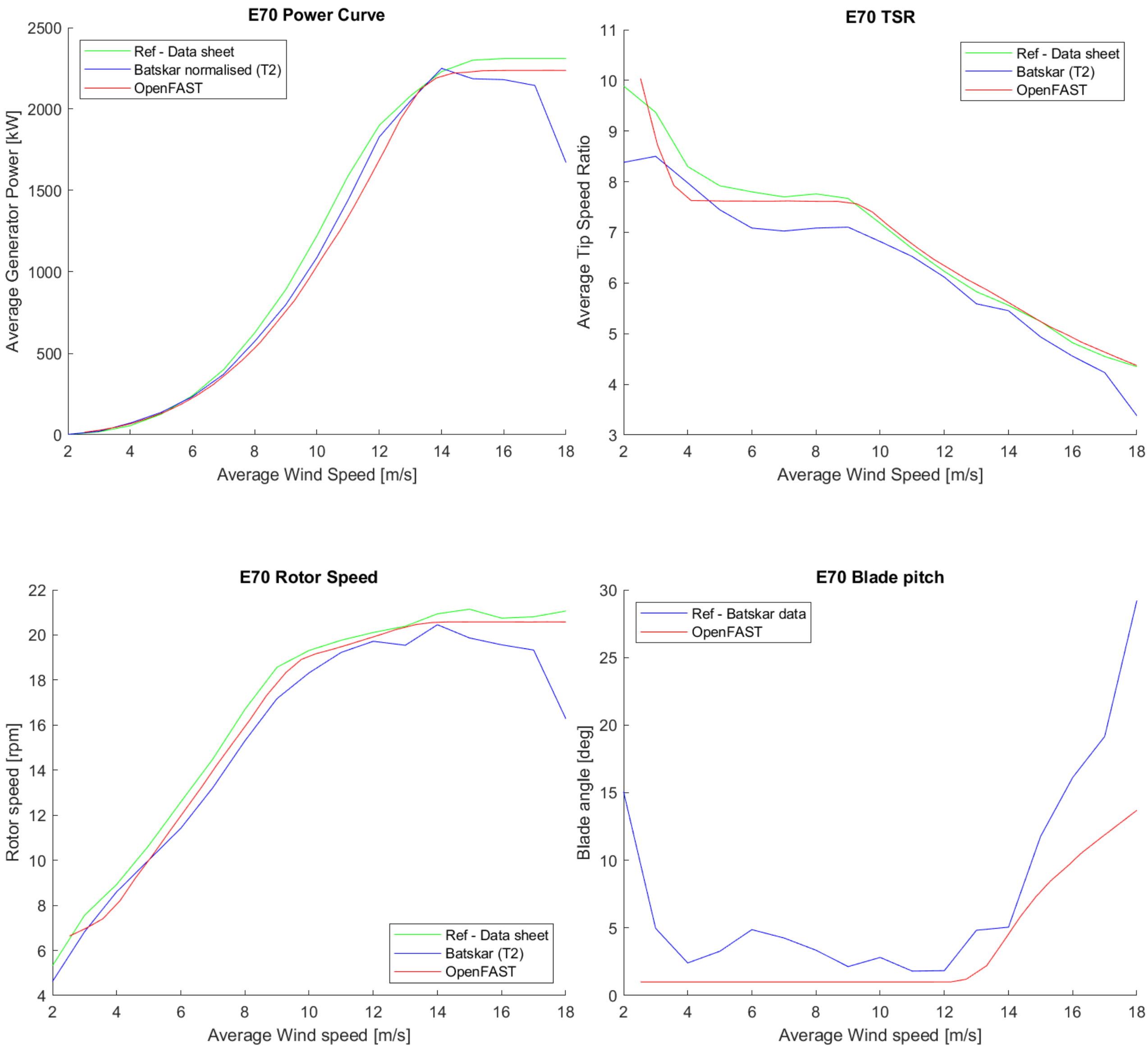

Figure 9. Enercon E70 validation with OpenFAST model.

Some initial tests with FAST.Farm focused on a couple of test points found in the experimental data recorded at Båtskär. These data points are for a wind farm configuration resulting from the wind coming from a north-easterly direction. The figure below illustrates the losses as a result of wake impingement affecting Turbine 2. Overall, there is good agreement between the experimental data points, labelled Båtskär T1 and T2, and the results from the simulations, labelled FAST T1 and T2.

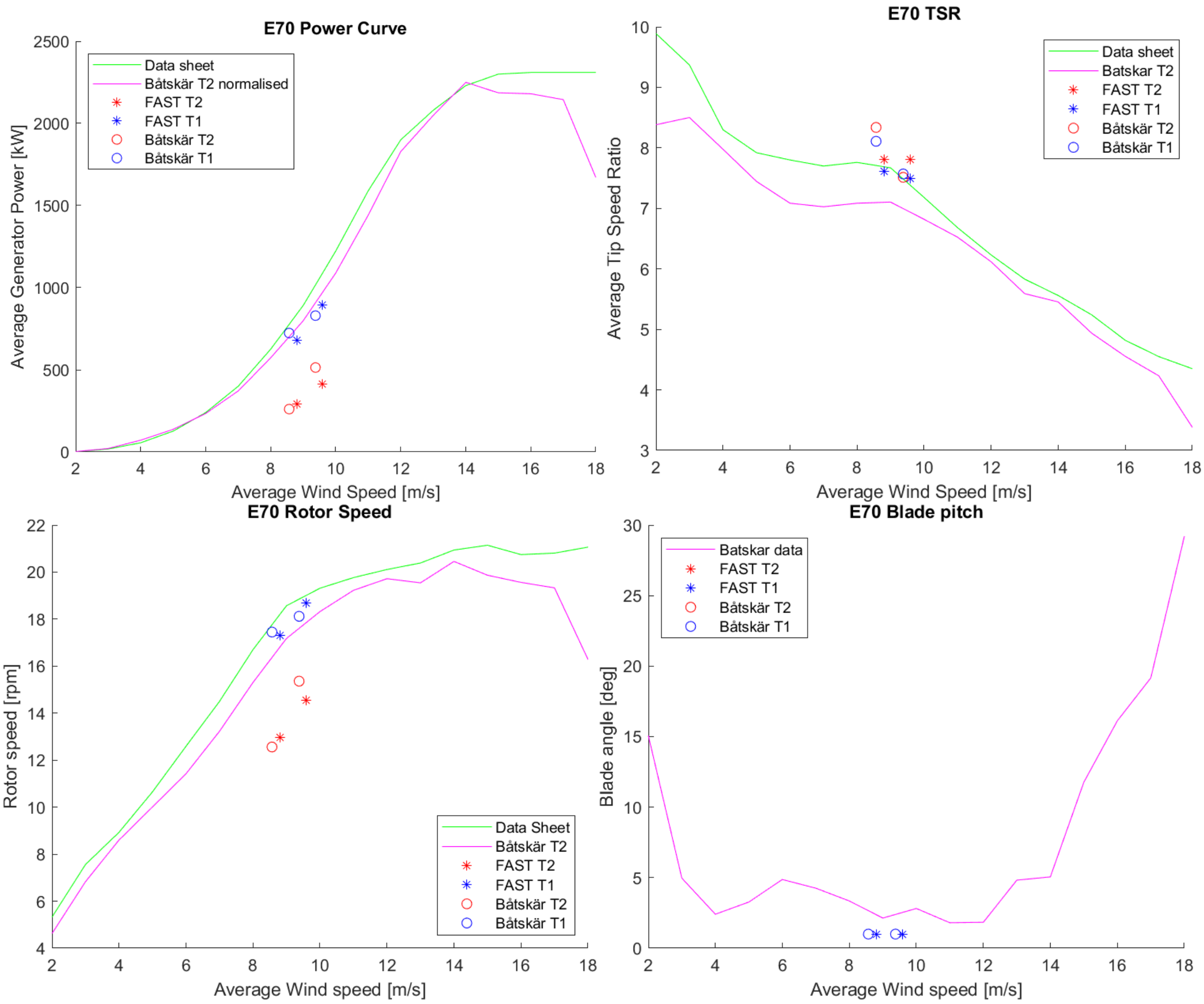

Figure 10. Båtskär full-impingement scenario (T1 impinges on T2).

The wind farm wide validation performed with FAST.Farm focuses on turbines 1 and 2. Given an analysis on the wind-rose for Båtskär, the dominant wind direction results in Turbine 1 lying in the wake of Turbine 2. This also aligns with the set of instrumentation installed in the wind farm. This validation draws attention to the losses associated with wake impingement.

In order to find a coherent set of data points to be simulated for the farm-level validation, several filters were applied to a compiled dataset with wake impingement information. A first screening of the data was by wind direction, which allows for filtering by the waked turbine desired for analysis. The time windows where there is wake impingement affecting Turbine 1 are then evaluated further to determine where quasi-steady conditions exist. These periods exclude the presence of gusts or other sudden changes in inflow conditions which are difficult to capture in a model. Of the remaining data points, the final simulation subset was created by applying filters for wind speed, shear and turbulence ranges.

A detailed validation will be included in a future publication.

5. Business case analysis

The current mainstream in controlling wind turbines is “each turbine for itself” i.e., each turbine is optimizing its own production without considering other wind turbines in the farm. More advanced control methods for optimizing and increasing the energy production of the whole wind farm, such as axial induction control and wake steering have been proposed and field tested. Promising results have been achieved in field tests implementing wake steering with increased energy production with turbines operated with wake steering control. IEA Wind TCP Task 44 has been established to coordinate international research in the field of wind farm control, VTT has participated in this task.

Considering the field tests carried out by the research community together with wind farm owners and operators, and the reported benefits of wake steering in optimizing and increasing the energy production of the whole wind farm, wake steering as a method was selected as bases of business case development. A spin-off with the working title TwinThrive and a proof-of-concept (POC) project implementing wake steering by this company was pursued within TUTTE together with Flexens and VTT.

5.1 Analysing wake losses

By wake effect we mean the influence of a wind turbine to the wind flow downwind of the turbine. This wake flow impacts the power production of downwind turbines within the wind farm. Power is lost due to decreased wind speed, and mechanical loads to the turbine are increased due to added turbulence which shortens turbine lifetime. Wake losses can be examined, and an estimate of the annual energy production lost due to wakes can be provided by analysing SCADA data available from the wind farm. This estimate works as a starting point when evaluating production gain potential by wake steering.

5.2 Increasing efficiency of wind energy

Field tests experimenting with wake steering have been conducted for example by NREL and Stanford. Increased production by turbines operated with wake steering have been reported among others by Fleming and Howland. [25]–[29]

Even though the research community has provided positive results from field experiments, according to the market survey conducted within TUTTE project, the original equipment manufacturers (besides Siemens Gamesa) have still not launched products for wake steering. Existing third-party products by companies such as breeze, bazefield, SentientScience and DNV-GL meant for analysing the production of a wind farm by connecting to the SCADA data produced by the wind farm.

5.3 Spinning-off TwinThrive

Given the clear benefits of and the lack of offering for wake steering, launch of a spin-off company TwinThrive was pursued. Flexens further developed the business plan and discussed with possible business partners. Freedom to operate was evaluated and seed funding searched for the prospective spin-off company, which would be formed together by the start-up team, Flexens, VTT and investors.

While reported research and development activities around the world showcasing the benefits from wake steering quite clearly indicate the increased energy production with the method, more trials and experiments are needed to gather further proof of the benefits but also information on the implications to fatigue loads and lifetime of the wind turbines within a wind farm operated in this way. Going forward with the aspirations to spinning-off a company in business with wake steering, it will be crucial to develop the capability of implementing and demonstrating the method in the field within an operational wind farm.

6. IEA collaboration

The project has enabled the technical contribution of VTT to the International Energy Agency Wind Technology Collaboration Program (IEA Wind TCP) in the period May / 2021 through September / 2022. The key outcomes are VTT contribution to IEA Wind TCP across Task 44, Task 46, Task 19 and Task 54; as well as VTT dissemination actions (IEAWIND kokouksen takeaway webinaari) to communicate in Finland the progress in deployment and technology advancement of wind energy. A more detailed description of this undertaking is presented in [30].

The participation of VTT in IEA Wind TCP technical activities developed in the Tasks has been key to progress in understanding of key challenges affecting wind energy technical maturity and competitiveness; as well as creating and maintaining a global network with industry and academic partners to develop solutions to address those challenges.

The effort committed to Task 19 “Wind energy in cold climates” has enabled the definition of a follow-up work programme through Task 54.

The technical participation in Task 44 “Wind farm flow control” has contributed to define key concepts and building blocks in the emerging topic of wind farm control; as well as to build the key industrial and academic connections to engage in future research.

Finally, the work in Task 46 “Erosion of wind turbine blades” has been key to understand the variability of rain characteristics across the globe, and the need for in-situ measurements at the wind farms to mitigate blade erosion by means of wind farm control. A key outcome has been the formulation of Horizon Europe Project AIRE, built to understand the atmospheric factors driving blade erosion. VTT participates with the objective of measuring in-situ the key atmospheric factors affecting erosion, with the objective of mitigating its effect.

7. Conclusions

Results of the analysis of the influence of atmospheric stability on wind farm efficiency suggest the stability metrics used in this work could potentially provide actual local information which can be beneficial for short term wake loss and production estimation. For more in-depth conclusions on this topic the reader is directed to [14].

Regarding the topic of wake losses, a method has been formulated to separate the contributions of orography and wake interaction in the overall efficiency of onshore wind farms.

The analysis showed how orography compensates significantly the effect of wakes in the wind farm, specifically and highlights the relevance of detailed site assessment when analysing prospective wind farm sites. Observed wake losses were around 10% of gross energy yield in the analysed wind farm (Santavuori), out of which 47% were estimated to be compensated by the effect of orography.

The analysis also stresses the limitations of the well-established wake engineering model by Jansen, which is not able to capture the qualitative dependency of experimental wake losses as a function of wind speed and wind direction. The best fitting wake decay coefficient for the Jansen model was 0.03 in Santavuori wind farm.

Icing conditions were analysed for the Santavuori site using VTTs icing atlas and the turbine SCADA data that was made available for the project. The main finding that was seen in the three-year SCADA dataset was that icing had a large year-over-year variance. This is relevant for icing condition assessment; basically, some kind of long-term analysis would be required to fully understand the icing conditions at the site. Using the IEA ice class as a reference, the ice class of the site was the same (IEA ice class 2) when looking at three-year average from SCADA and the 20-year average from the ice atlas.

These average icing conditions would mean on average roughly 250 hours of meteorological icing / year (2.9%) leading to production losses between 3 – 4 % annually. Most icing seems to occur at temperatures close to 0°C and at wind speeds below 7 m/s.

Future research in this field should aim towards more advanced wind farm performance analysis models such as FAST.Farm. In this context the research started in TUTTE will be continued in EU project AIRE "Advanced study of the atmospheric flow Integrating REal climate conditions to enhance wind farm and wind turbine power production and increase components durability" (2023-2027).

References

[1] P. Veers *et al.*, "Grand challenges in the science of wind energy," *Science (1979)*, vol. 366, no. 6464, Oct. 2019, doi: 10.1126/SCIENCE.AAU2027.

[2] R. W. Baker and S. N. Walker, "Wake measurements behind a large horizontal axis wind turbine generator," *Solar Energy*, vol. 33, no. 1, pp. 5–12, Jan. 1984, doi: 10.1016/0038-092X(84)90110-5.

[3] M. Magnusson and A. S. Smedman, "Influence of atmospheric stability on wind turbine wakes," *Wind Engineering*, vol. 18, no. 3, pp. 139–152, 1994.

[4] R. Gómez-Elvira, A. Crespo, E. Migoya, F. Manuel, and J. Hernández, "Anisotropy of turbulence in wind turbine wakes," *Journal of Wind Engineering and Industrial Aerodynamics*, vol. 93, no. 10, pp. 797–814, 2005, doi: 10.1016/J.JWEIA.2005.08.001.

[5] B. Sanderse, S. P. van der Pijl, and B. Koren, "Review of computational fluid dynamics for wind turbine wake aerodynamics," *Wind Energy*, vol. 14, no. 7, pp. 799–819, Oct. 2011, doi: 10.1002/WE.458.

[6] M. E. Rhodes and J. K. Lundquist, "The Effect of Wind-Turbine Wakes on Summertime US Midwest Atmospheric Wind Profiles as Observed with Ground-Based Doppler Lidar," *Boundary Layer Meteorol*, vol. 149, no. 1, pp. 85–103, Oct. 2013, doi: 10.1007/S10546-013-9834-X.

[7] K. Bhaganagar and M. Debnath, "Implications of stably stratified atmospheric boundary layer turbulence on the near-wake structure of wind turbines," *Energies (Basel)*, vol. 7, no. 9, pp. 5740–5763, 2014, doi: 10.3390/EN7095740.

[8] J. Nielson and K. Bhaganagar, "Using les to understand wake evolution during the diurnal cycle," *ASME International Mechanical Engineering Congress and Exposition, Proceedings (IMECE)*, vol. 7A-2015, 2015, doi: 10.1115/IMECE201552045.

[9] W. A. El-Askary, I. M. Sakr, A. M. AbdelSalam, and M. R. Abuhegazy, "Modeling of wind turbine wakes under thermally-stratified atmospheric boundary layer," *Journal of Wind Engineering and Industrial Aerodynamics*, vol. 160, pp. 1–15, Jan. 2017, doi: 10.1016/J.JWEIA.2016.11.001.

[10] L. Zhan, S. Letizia, and G. Valerio Iungo, "LiDAR measurements for an onshore wind farm: Wake variability for different incoming wind speeds and atmospheric stability regimes," *Wind Energy*, vol. 23, no. 3, pp. 501–527, Mar. 2020, doi: 10.1002/WE.2430.

[11] B. Du, M. Ge, C. Zeng, G. Cui, and Y. Liu, "Influence of atmospheric stability on wind-turbine wakes with a certain hub-height turbulence intensity," *Physics of Fluids*, vol. 33, no. 5, May 2021, doi: 10.1063/5.0050861.

[12] X. Han, D. Liu, C. Xu, and W. Z. Shen, "Atmospheric stability and topography effects on wind turbine performance and wake properties in complex terrain," *Renew Energy*, vol. 126, pp. 640–651, Oct. 2018, doi: 10.1016/J.RENENE.2018.03.048.

[13] W. C. Radünz *et al.*, "Influence of atmospheric stability on wind farm performance in complex terrain," *Appl Energy*, vol. 282, Jan. 2021, doi: 10.1016/J.APENERGY.2020.116149.

[14] M. Huttunen, T. Karlsson, R. Prieto, and S. Lele, "Atmospheric conditions and wind farm efficiency at two wind farms, onshore and offshore," unpublished, *VTT Technical Research Centre of Finland Ltd, Stanford University*, 2022.
[15] R. Prieto, T. Karlsson, M. Huttunen, J. Carreiro-Spencer, and A. Soininen, "On the quantification of wake losses and orography effect in onshore wind farms: an engineering approach," unpublished, *VTT Technical Research Centre of Finland Ltd, EPV Tuulivoima*, 2022.
[16] V. Lehtomäki *et al.*, "Available Technologies for Wind Energy in Cold Climates," Oct. 2018.
[17] S. Rissanen and V. Lehtomäki, "Wind Power Icing Atlas (WIceAtlas) icing map of the world," in *Winterwind Conference*, 2015.
[18] R. E. Bredesen *et al.*, "Recommended Practices report for Wind Energy Projects in Cold Climates," Feb. 2017.
[19] T. 19 IEA Wind TCP, "IEAWind-Task19/T19IceLossMethod: Method for estimating icing losses from wind turbine SCADA data," *GitHub*. 2018.
[20] J. Jonkman and K. Shaler, "FAST.Farm User's Guide and Theory Manual," 2021.
[21] J. M. Jonkman and M. L. Buhl, "FAST User's Guide," 2005. [Online]. Available: www.nrel.gov
[22] G. Bir, "User's Guide to BModes (Software for Computing Rotating Beam Coupled Modes)," 2005. [Online]. Available: http://www.osti.gov/bridge
[23] B. J. Jonkman, "TurbSim User's Guide v2.00.00," 2014. [Online]. Available: www.nrel.gov/publications.
[24] P. Fleming *et al.*, "SOWFA + Super Controller User's Manual," 2013. [Online]. Available: www.nrel.gov/publications.
[25] P. Fleming *et al.*, "Initial Results From a Field Campaign of Wake Steering Applied at a Commercial Wind Farm: Part 1," *Wind Energy Science Discussions*, pp. 1–22, Feb. 2019, doi: 10.5194/wes-2019-5.
[26] P. Fleming *et al.*, "Continued results from a field campaign of wake steering applied at a commercial wind farm - Part 2," *Wind Energy Science*, vol. 5, no. 3, pp. 945–958, Jul. 2020, doi: 10.5194/WES-5-945-2020.
[27] M. F. Howland, A. S. Ghate, S. K. Lele, and J. O. Dabiri, "Optimal closed-loop wake steering - Part 1: Conventionally neutral atmospheric boundary layer conditions," *Wind Energy Science*, vol. 5, no. 4, pp. 1315–1338, Oct. 2020, doi: 10.5194/WES-5-1315-2020.
[28] M. F. Howland *et al.*, "Optimal closed-loop wake steering - Part 2: Diurnal cycle atmospheric boundary layer conditions," *Wind Energy Science*, vol. 7, no. 1, pp. 345–365, Feb. 2022, doi: 10.5194/WES-7-345-2022.
[29] M. F. Howland *et al.*, "Collective wind farm operation based on a predictive model increases utility-scale energy production," *Nature Energy 2022 7:9*, vol. 7, no. 9, pp. 818–827, Aug. 2022, doi: 10.1038/s41560-022-01085-8.
[30] R. Prieto and T. Karlsson, "TUTTE Deliverable 8.1 Contribution to IEA Wind Technology collaboration program," 2022.

DocuSign

Certificate Of Completion

Envelope Id: 5BF7BCD952444EE1BF38A901CEF2B81E		Status: Completed
Subject: Complete with DocuSign: BF_TUTTE - Final report.pdf		
Source Envelope:		
Document Pages: 26	Signatures: 1	Envelope Originator:
Certificate Pages: 1	Initials: 0	Raul Prieto
AutoNav: Disabled		Vuorimiehentie 3, Espoo,
EnvelopeId Stamping: Disabled		., . P.O Box1000,FI-02044
Time Zone: (UTC+02:00) Helsinki, Kyiv, Riga, Sofia, Tallinn, Vilnius		Raul.Prieto@vtt.fi
		IP Address: 130.188.17.15

Record Tracking

Status: Original 04 November 2022 | 08:56	Holder: Raul Prieto Raul.Prieto@vtt.fi	Location: DocuSign

Signer Events	Signature	Timestamp
Raul Prieto Raul.Prieto@vtt.fi Teknologian tutkimuskeskus VTT Oy Security Level: Email, Account Authentication (None)	DocuSigned by: Raul Prieto FA1A895B52D447F... Signature Adoption: Pre-selected Style Using IP Address: 130.188.17.15	Sent: 04 November 2022 | 08:56 Viewed: 04 November 2022 | 08:56 Signed: 04 November 2022 | 08:57 Freeform Signing

Electronic Record and Signature Disclosure:
Not Offered via DocuSign

In Person Signer Events	Signature	Timestamp

Editor Delivery Events	Status	Timestamp

Agent Delivery Events	Status	Timestamp

Intermediary Delivery Events	Status	Timestamp

Certified Delivery Events	Status	Timestamp

Carbon Copy Events	Status	Timestamp

Witness Events	Signature	Timestamp

Notary Events	Signature	Timestamp

Envelope Summary Events	Status	Timestamps
Envelope Sent	Hashed/Encrypted	04 November 2022 | 08:56
Certified Delivered	Security Checked	04 November 2022 | 08:56
Signing Complete	Security Checked	04 November 2022 | 08:57
Completed	Security Checked	04 November 2022 | 08:57

Payment Events	Status	Timestamps